EPJ Photovoltaics **14**, 32 (2023)
© A.J. Carr et al., Published by EDP Sciences, 2023
https://doi.org/10.1051/epjpv/2023027

Available online at:
www.epj-pv.org

Special Issue on 'EU PVSEC 2023: State of the Art and Developments in Photovoltaics', edited by Robert Kenny and João Serra

Regular Article — Open Access

Thermal model in digital twin of vertical PV system helps to explain unexpected yield gains

Anna J. Carr, Ji Liu, Ashish Binani, Kay Cesar, and Bas B. Van Aken*

TNO Energy and Materials Transition – Solar Energy, Westerduinweg 3, 1755 LE, Petten, the Netherlands

Received: 2 July 2023 / Received in final form: 19 September 2023 / Accepted: 9 October 2023

Abstract. The business case of novel integrated applications of solar energy is often regarded as a straightforward extrapolation of standard solar parks. But when the design of the solar park is remarkably different from typical solar parks, the operating conditions of the PV panels could also be changed. We have applied the digital twin to an R&D location with nine rows of eight bifacial PV panels in a vertical east/west orientation with varying row-row distances. We simulated the in-plane irradiances, based on measured GHI, which turned out to be in good agreement with observations of in-plane irradiances. But, using default free-standing PV heat transfer coefficients, the modelled module temperatures were too high and the simulated module powers too low. Applying an in-house developed method, we found that the heat transfer coefficient Uc is nearly double, and the vertically placed modules operate at a much lower temperature. The adjusted value for Uc leads to a 2.5% higher annual energy yield and higher performance ratio, partially offsetting the energy loss due to the less than optimal configuration. In conclusion, the digital twin increased the understanding of the vertical PV system and support future decision making, for instance for the application of vertical PV in combination with agriculture, where the low ground coverage ratio of vertical PV matches well with the needs from the agricultural sector.

Keywords: Solar park / digital twin / vertical installation / thermal behavior / yield analysis

1 Introduction

The allocation of scarce land to agriculture, housing and renewable energy generation is a very topical and political issue and leads to demands for dual land use, like agrivoltaic systems [1–3]. The business case of novel applications of solar energy, particularly in integrated solutions, is often regarded as a straightforward extrapolation of standard solar parks. But the design of the integrated solar park could be remarkably different from typical solar parks in the same region. This could affect the operating conditions of the PV panels themselves. For example, vertical PV panels have very different daily generation profiles compared to low-tilt East-, West- or South-facing solar panels.

Digital twins are often used to support the operations and maintenance of utility-scale solar parks. The twins consist of a real PV system and a copy in digital format. The real part are the PV panels, weather station, power electronics, sensors and surroundings. The digital version mimics the output of the PV panels based on the time series of weather and other environmental data. The simulated values are compared to observed data. This takes place in near-real time for urgent issues or later in offline analysis of the performance.

The aim of this work is to show that digital twins, combining environmental and PV measurements in a real system with a virtual model describing the interaction of light and temperature with the solar panels, lead to a better understanding of the real system. This holds for the general operating conditions, answering questions like "*how much renewable energy does the system convert from sunlight?*", but also for deviations due to accidental damage or gradual degradation.

We present measured results taken on an R&D vertical installation with bifacial panels in the Netherlands. The digital counterpart is created in BIGEYE [4], TNO's in-house bifacial simulation software. For both direct and diffuse light, shading and ground-reflected light are taken into account. BIGEYE simulates the maximum power-point voltage and current. For that it also determines the operating temperature of the module. Finally, it reports the average in-plane irradiance for each module, separated in front and rear and the constituting components.

* e-mail: bas.vanaken@tno.nl

We will show validated time-series of simulated and measured in-plane irradiances, module temperatures and operating voltages. As far as we know, this contribution is the first to report on the real-life operating temperature of a vertical bifacial PV system. Previous work focused, for example, on the effect of module bill of materials [5], [ambient] temperature-dependent energy gain [6] or cost effectiveness [7]. Based on these comparisons, we deduced that the vertical PV panels operate at lower temperature than expected for *standard* free-standing PV based on default heat transfer coefficient values. We also present aggregated daily energy generation and show that the expected annual energy yield is 2.5% higher due to the lower operating temperature.

2 Methods

2.1 Real twin – physical set-up

A vertical PV system is installed, located near the TNO facilities in Petten, the Netherlands, with nine rows of eight bifacial PV panels in a vertical east/west orientation. The spacing between module rows is 2, 4 or 6 m. For most modules, the front and rear side of the modules face West and East, respectively. Some are installed the other way round. Various crystalline Si n-type cell technologies and module bills of materials are installed. Most PV panels in our system are standard, glass-glass modules with nominal power of 315 Wp with an estimated transparency of 6.6% due to the lack of white scattering material around the cells' edges. They contain 60 n-type M2 solar cells with TOPCon technology. The 72 PV modules are individually optimized with SolarEdge power optimizers. In addition, global horizontal irradiance, east- and west-facing plane of array irradiance and ambient and module temperatures are recorded in 5 min intervals.

Figure 1 shows the overview of our vertical PV system. Both real and virtual versions of the twin are shown. We focus here on the second row from the top, East side, with 6 m distance on both sides to the next module row.

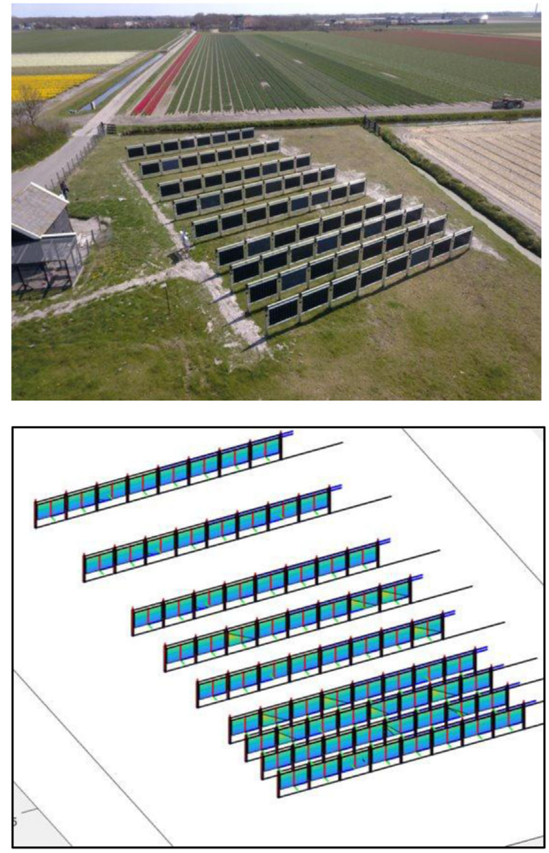

Fig. 1. Photograph of the real part of the vertical PV system twin (top). MATLAB generated drawing of the virtual part of the twin, including horizontal and vertical construction elements (bottom).

2.2 Digital twin – BIGEYE software

The digital counterpart is created in BIGEYE [4]. BIGEYE is a state-of-the-art tool developed by TNO to simulate the performance of PV systems, with a focus on bifacial systems [8,9]. BIGEYE deploys the Erbs model [10] to estimate diffuse horizontal irradiance (DHI) from global horizontal irradiance (GHI) when DHI is not available. BIGEYE uses the Perez model [11] to break down DHI into sky dome and circumsolar components, and to assess horizon brightening and darkening.

BIGEYE implements a 3D view factor model to accurately handle the ground and other diffuse reflectors, for instance, the irradiance from the ground to, in case of vertical PV, both sides of bifacial modules. Therefore, in vertical, bifacial systems, elements of the support structure are more likely to cast shades on a light receiving surface of the module than in conventional systems. BIGEYE has flexibility in simulating such shades, and their impact on the IV curves (mismatch) of modules and strings. Amongst others, it takes into account the division of the modules in blocks of cells protected by by-pass diodes [9].

Shading due to the vertical poles and horizontal beams is taken into account, as is the ground-reflected light due to the albedo of the grass between and below the rows. BIGEYE calculates the irradiance per cell, including hard shading and inhomogeneities, and determines the corresponding IV-curve of that cell. The module IV-curve is extracted by combining the, in this case, 60 individual cell IV-curves by current matching. From the full module IV curve, the maximum power-point is calculated and thus maximum power-point voltage and current are determined. For that it also determines the operating temperature of the module in the ambient conditions. Finally, it reports the in-plane irradiance for each module and timestep, separated in front and rear and the constituting components: beam, circumsolar, diffuse sky, horizon and ground-reflected.

2.3 Heat transfer coefficient Uc determination

We calculated weighted irradiance based on previous irradiance measurements to compensate for the thermal mass and slower thermal response of the module [5]. Based on ambient temperature and the weighted, in-plane

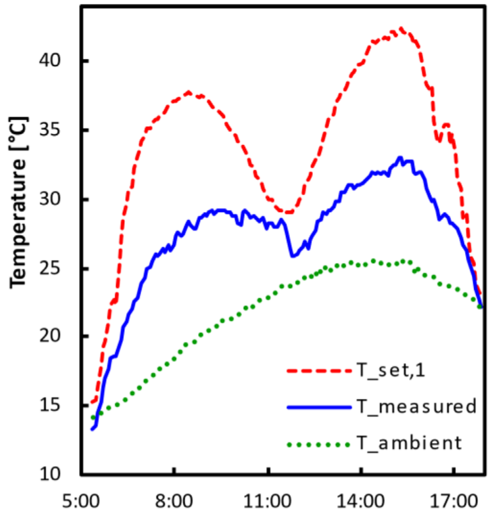

Fig. 2. Daily profile of the module temperature: blue solid line shows observed temperatures, red dashed line presents modelled ones, and green dotted line displays ambient temperatures.

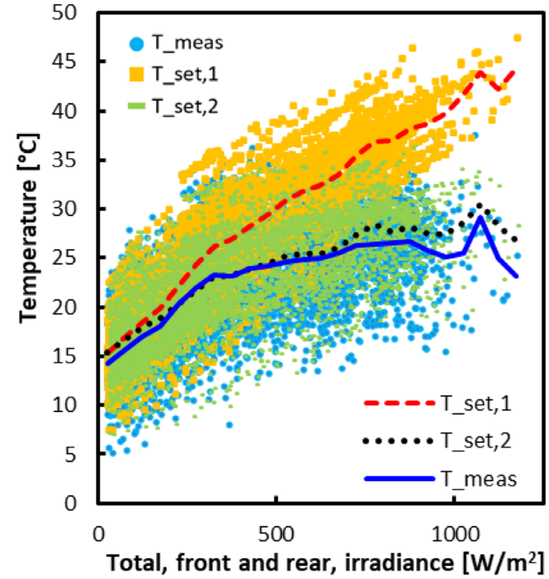

Fig. 3. Observed and modelled module temperatures. *T_meas* are the observed values; *T_set,1* are modelled using $U_c = 29\,W/m^2/K$ and *T_set,2*, using $U_c = 56\,W/m^2/K$. Lines are average temperatures per $50\,W/m^2$ irradiance bin.

irradiance for each data point, we calculate the root mean square errors RMSE of the calculated module temperature minus the measured module temperature for a range of values for the heat transfer coefficient U_c.

3 Results

3.1 Module temperature and operating voltage

The electrical performance of the modules is modelled using 1-diode parameters, fitted to I-V measurements under standard test conditions. For the module temperature, the steady state model is used, similar to PVsyst. The standard heat transfer coefficient value for open rack mounting, that is $U_c = 29\,W/m^2/K$, is used with label "*set,1*" [12]. In Figure 2 the measured and modelled module temperature for a sunny day in September are given. Note that due to the vertical positioning of the solar panels, the irradiance on the panels is low around solar noon, causing an obvious reduction in module temperature. Clearly, the observed module temperatures are much lower than the modelled values for the module temperature.

Looking at a larger dataset of observed module temperatures and total in-plane irradiance, front and rear, we find that a U_c of $56\,W/m^2/K$ gives the best agreement between observations and modelled module temperatures. For simulations with the updated value, the label "*set, 2*" will be used. We plot the module temperature also as function of the total, front and rear, in-plane irradiance for the period 26 August to 4 October 2022 in Figure 3. Because of the large number of data points, we also calculate the average module temperature per $50\,W/m^2$ irradiance bin and plot these as thick lines. The root mean square error, RMSE, for the default and updated values compared to the measured values are, respectively, 9.9 and 1.5. Clearly "*set,2*" is in much better agreement with the measured data than the original model.

Figure 4 shows the corresponding operating voltage. Although there are some differences between "*set,2*" and measured values, the fit is much better than for the original model. In particular, at higher total in-plane irradiances, the operating voltage for the original model decreases due to the prominent increase in module temperature, whereas for both measured and "*set,2*" the decrease in voltage due to increasing module temperature is more or less compensated by the increase in voltage due to increasing irradiance.

Note: near the maximum power point, the P-V curve is nearly flat. That means that at an operating voltage that is ±1% different from the maximum power voltage will lead to only a −0.1% loss in power. Also in an outdoor set-up, the conditions are constantly varying, making the measured operating voltage an approximation of the maximum power point voltage. The agreement between observations of power optimizer voltage and modelled maximum power point voltage with *set,2* shows a root mean square error of 0.5 compared to the RMSE of 1.3 for the default value in *set,1*.

3.2 Effect on daily energy

Finally, we look at the daily generated electricity. Plotting the modelled daily energy using the default and updated U_c values against the observed daily energy, we find a very good correlation, as seen in Figure 5. For the default U_c the slope of modelled versus observed daily energy is 0.95, for the updated value the slope is even closer to unity, namely 0.99. Note that the U_c is updated to reflect measured module temperatures and is not fitted against hourly power or daily energy performance.

In Figure 6, we plot the relative increase in daily energy, comparing the model with the updated value for the heat transfer coefficient Uc to the default value, as function of

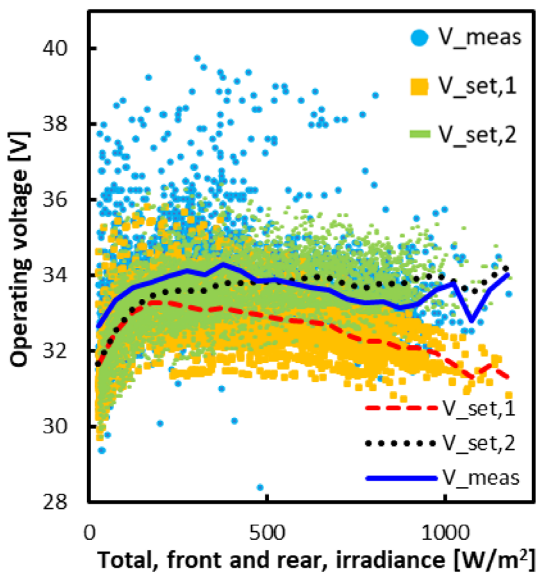

Fig. 4. Observed and modelled operating voltage. *V_meas* are the observed values; *V_set,1* are modelled using $U_c = 29\ W/m^2/K$ and *V_set,2*, using $U_c = 56\ W/m^2/K$. Lines are average operating voltages per $50\ W/m^2$ irradiance bin.

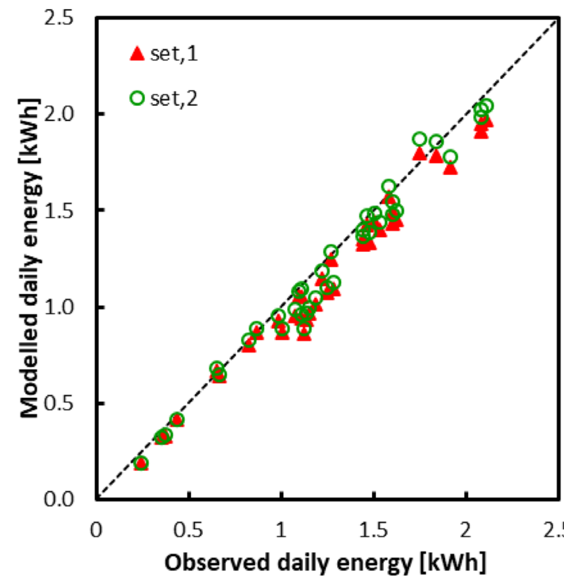

Fig. 5. Modelled daily energy against observed daily energy for *set,1* using $U_c = 29\ W/m^2/K$ and *set,2*, using $U_c = 56\ W/m^2/K$. The dashed line indicates $y = x$.

the observed daily energy. There is a clear trend that with increasing observed daily energy, the relative increase also increases. At the days with the highest observed daily energy yield, the relative increase is as high as 4%. Obviously, the observed daily energy yield will be highest for days with high total irradiance. Under these high total irradiance conditions, the modules will also absorb a lot of heat, both from infrared heating and from the excess energy in the photovoltaic conversion. As a result, for these days the temperature difference between modules that operate with different heat transfer coefficients will be highest. Consequently, the modules with the higher heat transfer coefficient will have the largest increase in energy conversion on days with the largest irradiance and largest daily energy.

We have checked whether the results in Figure 6 depend on factors such as day light length or ambient temperatures. When comparing hourly values of the relative difference and the observed energy, the same trend is observed: a linear increase at low energy, followed by a broader cloud. We note a small deviation from linearity at higher energies towards a lower slope.

The ambient temperature does make a minor difference: data points with higher ambient temperature tend to have higher relative differences compared to data points corresponding to lower ambient temperature at comparable observed energies.

For the calendar year 2022, the whole system, including row-row spacings of 2, 4 and 6 m, various cell and module types and a mixture of sunny side West and sunny side East orientations, produced 22.2 MWh with an installed nominal capacity of 22.6 kWp, thus nearly 1000 kWh/kWp. Unfortunately, the system was down for a period of six weeks in March and April with an estimated production loss of about 2 MWh. The specific AC yield for the panels with the spacing of 6 m was actually as high as 1100 kWh/kWp, not taking into account the lost production weeks. As the

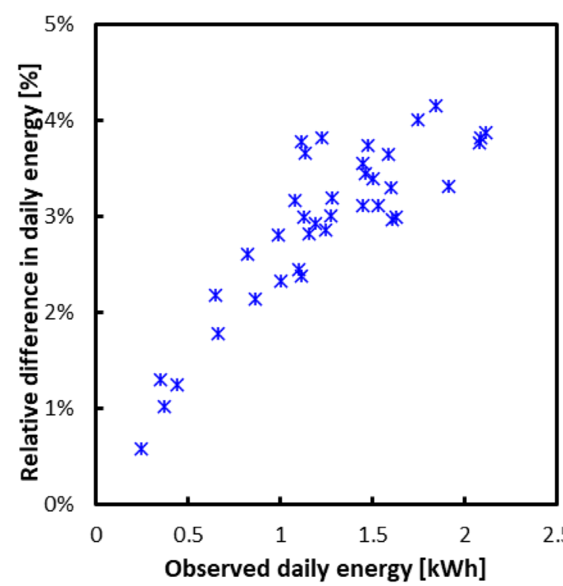

Fig. 6. Relative increase in daily energy for the updated value, $U_c = 56\ W/m^2/K$, compared to the default value.

considered year was exceptionally sunny in our region, we also have modelled the annual energy yield using Meteonorm data based on average climate data for 1990–2020. We find an annual DC energy yield of 1060 kWh/kWp for the vertical system with 6 m spacing with the updated Uc value contributing an additional 2.5%.

4 Conclusions

We present a detailed analysis of the digital twin of a vertical R&D installation with bifacial panels. We validated the time-series of simulated west-plane and east-plane irradiances, based on measured GHI, which turned out to be in good agreement with observations of in-plane irradiances. In contrast, using standard heat transfer coefficients for free-standing PV, the digital twin's module temperatures were too high, and consequently, the simulated module powers too low.

Applying an in-house developed extraction method, we found that the heat transfer coefficients U_c of these vertically placed modules are nearly double the default U_c values and operate at a temperature difference with respect to ambient that is nearly halved. The adjusted value for U_c lead to a 2.5% higher annual energy yield. Thus, the vertical modules operate at relatively low temperature with a higher performance ratio, partially offsetting the energy loss due to the less than optimal configuration. Project developers and everyone else involved in optimizing or evaluating the design of a solar park with vertical PV modules should consider the effect of the increased heat transfer coefficient for their business case.

In conclusion, the digital twin increased the understanding of the vertical PV system and supports future decision making, for instance for the application of vertical PV in combination with agriculture, where the low ground coverage ratio of vertical PV matches well with the needs from the agricultural sector.

This work contains results generated in the project SolarEcoPlus and is partially funded by a Topsector Energiesubsidie from the Dutch Ministry of Economic Affairs.

Author contribution statement

The authors confirm contribution to the paper as follows: study conception and design: B.B. Van Aken, I. Cesar; data collection: J. Liu, A.J. Carr; analysis and interpretation of results: A.J. Carr, A. Binani, B.B. Van Aken; draft manuscript preparation: A.J. Carr, B.B. Van Aken. Project management and funding: I. Cesar. All authors reviewed the results and approved the final version of the manuscript.

References

1. G.A. Barron-Gafford et al., Agrivoltaics provide mutual benefits across the food–energy–water nexus in drylands, Nat. Sustain. **2** (2019), https://doi.org/10.1038/s41893-019-0364-5
2. M. Trommsdorff et al., Combining food and energy production: design of an agrivoltaic system applied in arable and vegetable farming in Germany, Renew. Sustain. Energy Rev. **140**, 110694 (2021)
3. C. Dupraz, Preface: AgriVoltaics2020 conference launching agrivoltaics world-wide, AIP Conf. Proc. **2361**, 010001 (2021)
4. G.J.M. Janssen, B.B. Van Aken, A.J. Carr, A.A. Mewe, Outdoor performance of bifacial modules by measurements and modelling, Energy Procedia **77**, 364 (2015)
5. M.W.P.E. Lamers, E. Özkalay, R.S.R. Gali, G.J.M. Janssen, A.W. Weeber, I.G. Romijn, B.B. Van Aken, Temperature effects of bifacial modules: Hotter or cooler? Sol. Energy Mater. Sol. Cells **185**, 192 (2018)
6. M.T. Patel, R.A. Vijayan, R. Asadpour, M. Varadharajaperumal, M.R. Khan, M.A. Alam, Temperature dependent energy gain of bifacial PV farms: a global perspective, Appl. Energy **276**, 115405 (2020)
7. R. Kopecek, J. Libal, Bifacial photovoltaics 2021: status, opportunities and challenges, Energies **14**, 2076 (2021)
8. G.J.M. Janssen et al., How to maximize the kWh/kWp ratio: simulations of single-axis tracking in bifacial systems, in *Proceedings of the 35th European Photovoltaic Solar Energy Conference and Exhibition* (Nov. 2018), pp. 1573–1577
9. A.R. Burgers, BIGEYE – simulation under shadow conditions, presented at the *6th Workshop on Bifacial PV*, Amsterdam (Sep. 2019)
10. D.G. Erbs, S.A. Klein, J.A. Duffie, Estimation of the diffuse radiation fraction for hourly, daily and monthly-average global radiation, Sol. Energy **28**, 293 (1982)
11. R. Perez, R. Seals, P. Ineichen, R. Stewart, D. Menicucci, A new simplified version of the perez diffuse irradiance model for tilted surfaces, Sol. Energy **39**, 221 (1987)
12. PVsyst User Manual, section on Array Thermal Loss. https://www.pvsyst.com/help/index.html?thermal_loss.htmhttps://www.pvsyst.com/help/index.html?thermal_loss.htm

Cite this article as: Anna J. Carr, Ji Liu, Ashish Binani, Kay Cesar, Bas B. Van Aken, Thermal model in digital twin of vertical PV system helps to explain unexpected yield gains, EPJ Photovoltaics **14**, 32 (2023)